June 2006

An experimental approach to modeling the strength of canine teeth

Patricia W. Freeman
University of Nebraska-Lincoln, pfreeman1@unl.edu

Cliff A. Lemen
University of Nebraska-Lincoln, clemen2@unl.edu

An experimental approach to modeling the strength of canine teeth

P. W. Freeman & C. Lemen

School of Natural Resources and University of Nebraska State Museum, University of Nebraska–Lincoln, Lincoln, NE

Keywords

tooth fracture; canine strength; finite-element analysis; beam theory; modeling teeth; carnivore canines; tooth strength.

Correspondence

Patricia W. Freeman, School of Natural Resources and University of Nebraska State Museum, University of Nebraska, Lincoln, NE 68588-0514, USA.
Email: pfreeman1@unl.edu

Received 3 November 2005; accepted 3 May 2006

Abstract

The strength of canine teeth in several carnivores is found through direct fracture experiments. The average forces required to break the canines of adult animals are coyote 1170 N, red fox 533 N, bobcat 737 N and raccoon 512 N. Stresses created in teeth at the breaking load are predicted by finite-element analysis and beam theory. The ultimate tensile stress sustainable in these teeth is 338 MPa in adult animals. The large pulp cavity in the canines of young animals significantly weakens the bases of their teeth (by about 25%), but as the animal ages the pulp cavity decreases and has little effect on overall tooth strength. The tooth material of young of the year is significantly weaker than that from older animals (by about 35%). With the experimentally derived ultimate tensile stress, finite-element analysis can estimate the breaking load of canines for several carnivores. A significant allometric relationship exists between log of body weight and log of strength of tooth (slope=0.81).

Introduction

We measure the strength of canine teeth from selected carnivores with fracture tests and develop a method to predict the strength of canines based on morphology using beam theory analysis (BTA; see Popov, 1999) and finite-element analysis (FEA; see Mattheck & Burkhardt, 1990). We also find the allometric relationship between canine strength and body weight for mammalian carnivores. Van Valkenburgh & Ruff (1987) studied canine strength across Carnivora by equating a canine to a cantilever (a beam fixed at one end). Although an excellent study, these authors derive only a relative index of strength. One of our goals is to provide a method for calculating absolute tooth strength.

One conceptual issue that must be dealt with is a clear understanding of tooth strength. A tooth's structural strength deals with the maximum load (force) the tooth can withstand without breaking. However, structural strength must be considered as a set of strengths based on the direction and position of the load applied to the tooth. We define the structural strength, $S_{A,x,}$ as the largest anteriorly directed load (N) a tooth can withstand when the force is applied at position *x* along the posterior edge of the tooth (Fig. 1a). This study deals with the quantification of $S_{A,0.7}$, a load applied at 70% of length from the tooth's base. Other types of structural strengths such as resistance to breakage from posteriorly, axially or laterally directed loads are not considered. We use the 70% position to simulate where the predator has grabbed its prey with its teeth in a life or death tug-of-war. If the tooth is more deeply embedded, there is a shorter input force arm to the base, lower mechanical advantage and lower bending stresses so that a larger force is needed to break the tooth. Conversely, if the tooth is barely embedded in the prey, it might well tear or slip out of the wound in the struggle and a large bending stress is unlikely. We selected the load at an intermediate point, 70% of length, deep enough for a good grip in the flesh but still with a reasonably long input arm.

$S_{A,0.7}$ can be found experimentally by applying increasing force at the 70% position until failure. Once $S_{A,0.7}$ is found, BTA or FEA can be used to calculate the bending stress, typically assumed to be a tensile stress, experienced at the point of fracture. This tensile stress is an estimate of the greatest stress the tooth material can withstand without breaking and is called the ultimate tensile stress ($\sigma_{t,u}$). Ultimate tensile stress is synonymous with a material's tensile strength. Once we determine σt,u for tooth material, we can use BTA or FEA to predict the strength of teeth without the need to break them.

It is important to understand the difference between situational structural strength of the whole tooth, SA,x, and the strength of the material from which the tooth is made, the material property σt,u. To distinguish the two concepts, consider a steel bridge. The steel has a material property of strength based on the maximal stress ($\sigma_{t,u}$) it can withstand without failure, and the bridge has a structural strength based on the maximum load it can support. The structural strength of the bridge can be increased through better design or increasing the thickness of the steel trusses, but the $\sigma_{t,u}$ of the steel re-

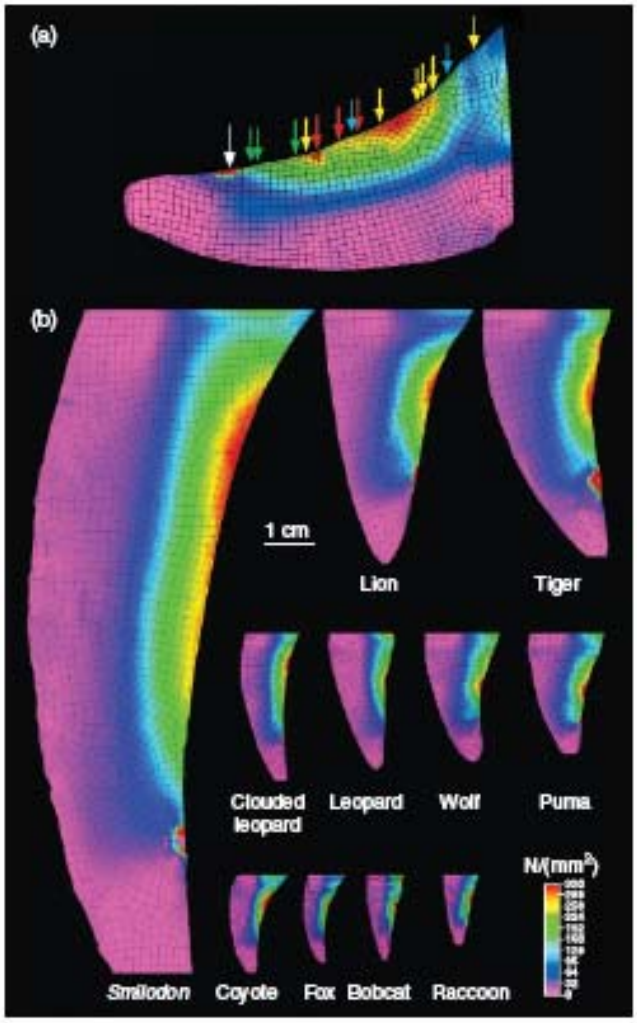

Figure 1 (a) Coyote canine in testing position illustrating the distribution of stresses as calculated by finite-element analysis (FEA) with a load of 1069N applied at a point 70% from the base (white arrow). Colored arrows show the relative position of tooth breaks for adult coyote Canis latrans (yellow), red fox Vulpes vulpes (red), bobcat Lynx rufus (green) and raccoon Procyon lotor (blue). (b) FEA mesh models taken from whole canine teeth showing the distribution of stresses. Teeth are drawn to scale, positionedwith the nose of the animal to the left and load applied from the right. Squared tips are an artifact of illustration. The scale in the lower right corner is the amount of maximum principal stress (tensile) at different parts of the teeth for the entire figure.

the same. Alternatively, the original design of the bridge could be kept and the strength of the bridge increased by substituting a steel alloy with a higher σt,u. Both FEA and BTA allow the prediction of a bridge's structural strength based on the material properties of steel and the bridge's design.

Teeth are made up of two hard materials: enamel and dentin. Although we gained interesting insights from our analyses of the tooth as a composite, ultimately complications forced us to abandon this line of enquiry and treat the enamel and dentin of the tooth as a single hypothetical homogeneous material (HHM). What this means is that we will be calculating a hypothetical ultimate stress, σt,hu. This simplification still allows us to make quantitative predictions of tooth strength.

Although beam theory is well documented in engineering texts (Popov, 1999), a short explanation here is useful. Consider a 20 mm coyote canine tooth that is loaded at the 70% position (14 mm from the base). When the load reaches 1000 N, the tooth breaks at a point 4 mm from the base. Therefore, the bending moment M at the point of fracture is 10 000 N mm (M=load × input arm). The bending stress, which in this case is an estimate of $\sigma_{t,u,}$ is calculated by the equation

$$\sigma_{t,u,} = \frac{Mc}{I} \quad (1)$$

where c is the perpendicular distance from the tooth's cross-section centroid to the section's extreme at the point of fracture and I is the moment of inertia of the cross section. Note that the critical stress point for tooth material is assumed to be in tension. Therefore, the extreme point on the section always refers to the posterior edge of the tooth that is in tension. In many cases tensile strength is more important than compressive strength because many structures tend to fail in tension. This is true because tensile strength is generally lower than compressive strength in brittle materials (Gordon, 1984). Data from the literature indicate that this generalization holds for both enamel and dentin (Craig & Peyton, 1958; Craig, Peyton & Johnson, 1961; Bowen & Rodriquez, 1962; Sano et al., 1994). The compressive strength of enamel in humans of 384 MPa is about 12 times greater than its tensile strength of 30 MPa; the compressive strength of dentin is 297 MPa and nearly three times higher than its tensile strength of 105 MPa.

FEA has been used extensively for the analysis of stress in teeth (Yettram, Wright & Pickard, 1976).This method requires an accurate model of the whole tooth in three dimensions and not just a single cross section. In the modeling phase of the analysis, the initial three dimensional (3-D) model is used to construct a mesh of lines, areas or solids (bricks or tetrahedrons). This mesh is used to make predictions about stresses created by an applied load. FEA is an alternative to the beam theory approach for the calculation of stresses, and in simple cases the two methods will generate similar results. However, beam theory, strictly speaking, assumes a straight, constant cross section beam. It has been found that if the beam varies gradually through its length, no significant errors in stress calculation are likely (Popov, 1999). But serious problems of stress concentration can be expected when abrupt changes occur in the shape and size of the cross section along the length of the beam. Classic examples of such abrupt changes from engineering are notches, grooves and bolt holes. FEA makes no such assumptions about the straightness or the constancy of the cross section and is a more gen-

eral analytic tool. Inclusion of the computationally more difficult but analytically superior FEA allows us to verify whether the simpler BTA is adequate for the analysis of these teeth.

Materials and methods

Study animals

Because dentin continues to be laid down after tooth eruption and may change in mechanical properties, we modeled young (6–8-months old) and older animals separately (Fig. 2a). All animals were salvaged fresh from a fur buyer dealing with wild-caught animals. All animals were killed in late December 2004 to January 2005, and all teeth were kept moist. Species included in our analysis were raccoon *Procyon lotor* (n=2), red fox *Vulpes vulpes* (n=3), coyote *Canis latrans* (n=7) and bobcat *Lynx rufus* (n=3). Museum specimens included a single individual each of lion *Panthera leo*, tiger *Panthera tigris*, leopard *Panthera pardus*, puma *Puma concolor*, clouded leopard *Neofelis nebulosa*, gray wolf *Canis lupus* and the saber-tooth *Smilodon floridanus*, and were used to create models of teeth only. These teeth were not broken. Weights for all species were taken from averages in Van Valkenburgh & Ruff (1987).

Creating the models

To use BTA or FEA, a model of the tooth's cross section or the whole tooth must be made. For the species we tested in the lab (red fox, coyote, raccoon and bobcat), we created models by sectioning fresh teeth every 0.635 mm to the level of the bone with an Isomet low-speed saw (Buehler, Lake Bluff, IL, USA). We drew the cross sections under a Wilde dissecting microscope equipped with camera lucida. In each drawing the layers of enamel, dentin and pulp cavity were outlined. The drawings were scanned into a computer, and the outlines of each layer were digitized. We used outlines based on 40 points to produce an accurate model of each section. For FEA these data were used in the Rhinoceros CAD program (version 3, Robert McNeel & Associates) to produce a 3-D model of the tooth. Each composite model consisted of layers of enamel, dentin and the pulp cavity vacuity. The tooth model was imported into FEMPRO (version 18.1, ALGOR) for a static mechanical analysis to produce a brick mesh model (Fig. 1b). The connection between the enamel and dentin layers was assumed to be bonded so that nodes were shared over the entire contact surface. Each of the teeth modeled for FEA as a composite of enamel and dentin was also modeled with these layers fused as a single HHM.

For BTA the cross section at the point of fracture was used to calculate the moment of inertia based on the arbitrary cross-section method (see below and Popov, 1999, pp. 401–405). These sections were digitized as described above; however, in all cases we used the HHM model.

For the museum specimens in the study, we constructed cross sections and models using front and side

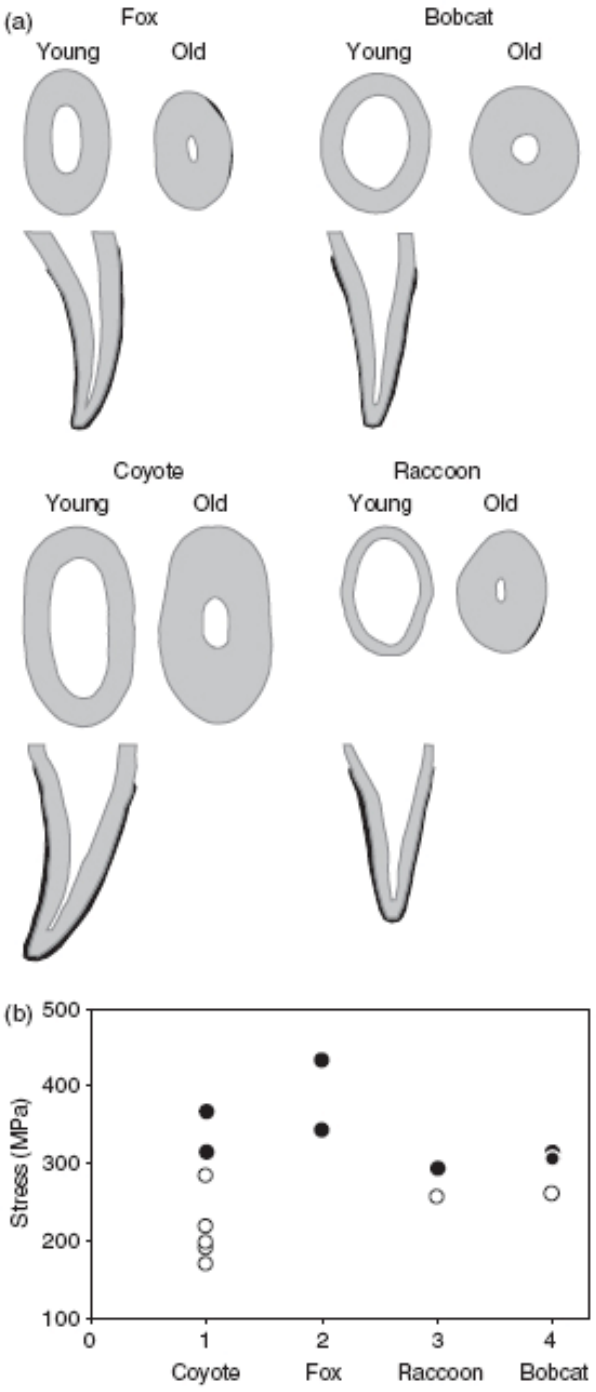

Figure 2 (a) A comparison of pulp cavities of young and old canine teeth. Cross sections near the base where the enamel ends show the larger cavity in young teeth and the narrower one in old teeth. Longitudinal sections are of young only. Enamel is black and dentin gray. Note that the enamel layer is quite thin. (b) Est mated tensile stresses at the point of fracture for adults (solid circles) and young (open circles) by species. These stress values were calculated using beam theory analysis under the hypothetical homogeneous materialassumption and are estimates of $\sigma_{t,u,}$.

ed leopard and gray wolf). We determined major and minor axes of ovals along the shank of the tooth from the

digitized images. Cross sections of these canines closely followed an oval and hence little information was lost with this assumption. We used this method because no tooth was available for destruction. Finally, we constructed a model of the saber-tooth S. *floridanus* by sectioning a cast of a complete canine. Cross sections of this tooth varied enough from oval that it was necessary to model the sections more accurately. This model, as with the other models generated for the museum specimens, was constructed using the HHM assumption and with no pulp cavity. No composite model could be constructed because we had no details about enamel thickness or size and placement of the pulp cavity (Fig. 1b).

Young's modulus of enamel and dentin

FEA requires Young's modulus of enamel and dentin when a composite model of tooth structure is used. Young's modulus (also known as the modulus of elasticity) is the slope of the straight-line portion of the stress–strain diagram. A high Young's modulus means a material requires a great force per unit area (stress) to produce a relatively small lengthening (strain). Young's modulus is important in analyses of structures composed of two or more materials because the elasticity of the different materials will impact the distribution of stresses.

We could not find estimates of Young's modulus for enamel and dentin in the species of carnivores used in this study. Estimates from humans were used and are 63.6 GPa for enamel and 19.7 GPa for dentin (Marshall *et al.*, 2001). We assumed that both dentin and enamel are isotropic in this study (see the Discussion for the possible role of anisotropy in enamel).

Mounting and breaking of teeth

We removed upper canines from the skulls of wild-caught carnivores and imbedded them to the canine-maxillary level into Die Stone (a gypsum casting product with high strength) held by a small length of 12.7 or 19.05 mm copper pipe, depending on the size of the canine. We broke the imbedded canine with an Instron testing machine by applying force to the posterior edge of the tooth with a steel indenter at a point 70% of the tooth's length from the level of imbedding. The Instron testing machine's speed of loading was set at 1 mm min^{-1}. To avoid large stresses where the indenter meets the tooth, we inserted a leather pad (thickness=1.6 mm) to spread the load. The relative positions of tooth fractures obtained during our breaking experiments are shown in Fig. 1a. Breaking bobcat teeth was problematic because the teeth tended to break at the indenter. This may have occurred because a crack was initiated by the indenter. In these cases the enamel was crushed at the point of load even with a leather pad. Such crushing obviously created cracks of unknown lengths in the tooth, and because of the central role of cracks in fracture mechanics these data could not be used because we had artificially weakened the tooth.

Calculating stress at the point of fracture

To calculate the ultimate bending stress ($\sigma_{t,hu}$) at the point of failure, we recorded the load needed to break the tooth and the location where the load was applied. We glued the broken tooth and sectioned it at the point of breakage to determine the cross section. From this we derived *c* and *I* to use in equation (1) to calculate the bending stress at the point of failure with BTA under the HHM assumption.

The equation for the moment of inertia involves the integration of a calculus equation that can be solved for many regular geometric shapes such as rectangles, circles and ovals. For biological shapes, such as tooth cross sections, this calculus problem cannot be solved. The value of *I* must be estimated either by assuming that the tooth's cross-sectional shape is a regular geometric shape that allows the equation to be solved for *I* (an oval was assumed by Van Valkenburgh & Ruff, 1987) or by using a discrete method to estimate *I*. We opted for the discrete approach by dividing the section into a large number of small squares of equal area *a* and calculating the perpendicular distance *y* from each small area's centroid to the cross-section centroid. Then the moment of inertia can be estimated using the equation $I=\Sigma y2a$. This approach can be used for any arbitrary cross section with or without vacuities (in our case we modeled the pulp cavity as a vacuity, which adds nothing to the strength of the tooth). The error of the discrete estimate can be made arbitrarily small by selecting smaller values for *a*. The problem is particularly easy on the computer, where a cross section can be represented as a series of square pixels in an image. The area *a* of each pixel and the accuracy of the outline are controlled by the scale of the image. By creating images of rectangles, circles and ovals, we found less than a 1% error between the discrete and continuous methods of calculations. A Windows-based computer program for the calculation of *I* from a cross-sectional image is available from the authors.

An alternative approach to BTA is FEA. In some cases the whole tooth was sectioned by the method described above to create an accurate model of the tooth. Using this model we performed FEA. Following the suggestion of Popov (1999) for working with brittle material, we used the maximum principal stress.

Finding $S_{A,0.7}$

The structural strengths of teeth were found in two very different ways in this study. Most obviously it was determined directly by breaking teeth and directly reading load values from the Instron machine. Data from these experiments allowed the calculation of σt,hu. Using σt,hu for our hypothetical tooth material, we modeled $S_{A,0.7}$ for species for which there are no breaking data. We used FEA to determine the lowest value of $S_{A,0.7}$ that was necessary to produce a $\sigma_{t,hu}$ of 338 MPa somewhere in the tooth. Using sectioning algorithms within FEMPRO, we

searched for the largest tensile stress throughout the tooth. Under the HHM model, maximal tensile stress was always found on the surface of the posterior edge of the tooth.

Results

Finding SA,0.7 experimentally

The average $S_{A,0.7}$ values for adult animals by species are coyote=1170 N (*n*=2), red fox=553 N (*n*=3), bobcat=737 N (*n*=2) and raccoon=512 N (*n*=1). The average $S_{A,0.7}$ values for young of the year by species are coyote=644 N (*n*=5), bobcat=409 N (*n*=1) and raccoon=359 N (*n*=1).

Finding $\sigma_{t,hu}$

We estimated stress in the hypothetical homogeneous tooth material using BTA based on our values of $S_{A,0.7}$. Stresses at failure points for the four test species are shown in Fig. 2b. Across all species our estimate of σt,hu averages 338 MPa (sd=48, coefficient of variation = 14%) for adults and 221 MPa for young of the year. The difference between adults and young is highly significant (*t*=4.56, P<0.0004, adult *n*=8, young of year *n*=7). Stress at failure is 35% less in young animals. It should be noted that our estimate of $\sigma_{t,hu}$ is a material property of tooth material in young and older animals and is not attributable to structural differences caused by the larger pulp cavity in younger animals (Fig. 2a). The cross sections for both young and old animals include the vacuity formed by the pulp cavity, with the result that the cavity affects our estimate of the moment of inertia and hence $\sigma_{t,hu}$.

In addition to weaker dentin, the teeth of young carnivores are weaker because of a larger pulp cavity. Mammalian teeth have a central pulp cavity that runs much

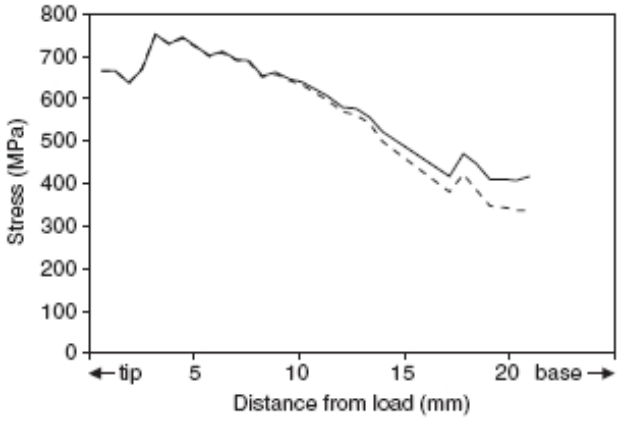

Figure 3 Impact of the pulp cavity on stresses in a young coyote tooth (solid line) and a simulated tooth created by mathematically filling in the pulp cavity (dashed line). Stress estimates are calculated with finite-element analysis under the hypothetical homogeneous material assumption and with a 1000N force applied to the tip (at the left of the graph). Note that stress values are similar in real and simulated teeth near the tip, where there is little or no pulp cavity. Near the base of the young tooth the pulp cavity is relatively large and has a higher stress than that found in the mathematically filled tooth. This means the young tooth is weaker at the base than its simulated twin.

of the tooth's length. With age this cavity decreases with the addition of dentin (Knowlton & Whittemore, 2001; Fig. 2a). To determine the impact of the pulp cavity on stress values, we used BTA to calculate stresses of a young coyote's tooth and stress in a virtual tooth. We created the latter with identical external morphology but with the pulp cavity completely filled. In comparing the stresses in these teeth, we found that the pulp cavity has little effect on the strength of the tooth except near its base (Fig. 3). The strength at the base of the tooth is reduced by about 20% by the presence of the large pulp cavity found in young coyotes of this age. Analysis for a young raccoon showed a reduction of 27% in strength. The pulp cavity is a narrow tube in adult animals. Once again, by comparing stresses in an adult tooth and its virtual twin, we found that the reduction in strength caused by the pulp cavity is much smaller in adults and did not exceed 1% in our species. Therefore, while the large pulp cavity in young animals significantly weakens their teeth, the pulp cavity problem can be reasonably ignored in adult animals.

The cumulative effects of lower dentin strength and a larger pulp cavity reduce the strength of the base of the juvenile tooth by almost half (48%). This reduction is so large that data from young of the year and adult specimens cannot be combined when studying tooth strength.

Modeling the strength of teeth

On the basis of FEA, we estimated the strength of the canines (of several species) that we never broke: lion 8243 N, tiger 7440 N, leopard 2483 N, puma 2840 N, clouded leopard 1229 N, gray wolf 2660 N and the saber-tooth 7000 N.

Combining our experimental values of SA,0.7 with the calculated values from FEA of museum specimens, we modeled the log–log relationship between body weight and tooth strength with a standard linear regression (Fig. 4; slope=0.81, intercept=2.06, P<0.001, R^2=0.99). Because the saber-tooth shape of *Smilodon* is vastly different, we excluded this species from the regression analysis bu t plotted the point in Fig. 4.

Comparing BTA and FEA

The differences between BTA and FEA can be illustrated with analysis of predicted stresses in a coyote tooth (Fig. 5). The largest differences, consistent across all teeth analyzed, are the high stresses predicted near the load point by FEA and the relatively low stresses predicted by FEA near the tooth base. Both FEA and BTA predict that high stresses are found in the middle of the tooth (about 30–60% of length) when the load is at the 70% point of the tooth. In this middle region, stresses are similar and high.

Discussion

The enamel and dentin problem

When a tooth is modeled as a combination of enamel and dentin, loads create much greater stresses in the

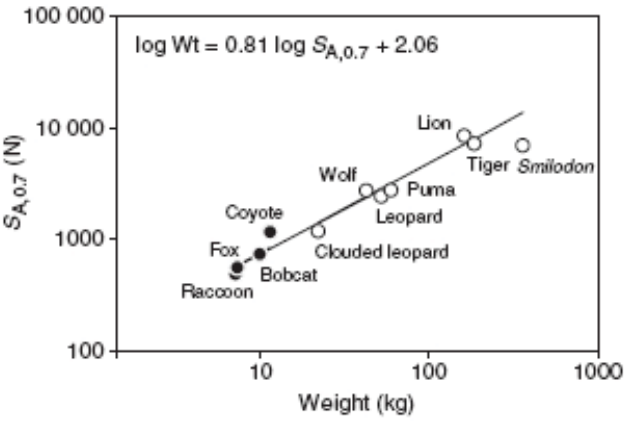

Figure 4 Allometric relationship between the log of body weight and the log of SA,x. SA,x is found experimentally for the raccoon Procyon lotor, red fox Vulpes vulpes, coyote Canis latrans and bobcat Lynx rufus (solid circles). For the lion Panthera leo, tiger Panthera tigris, puma Puma concolor, clouded leopard Neofelis nebulosa, leopard Panthera pardus, gray wolf Canis lupus and the saber-tooth Smilodon (open circles), SA,x is calculated using finite-element analysis under the hypothetical homogeneous material assumption.

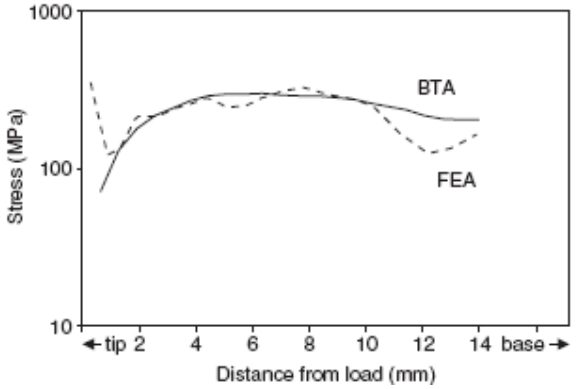

Figure 5 Comparison of stresses in an adult coyote tooth with a 1000N load applied at the 70% position predicted with beam theory analysis (BTA; solid line) and finite-element analysis (FEA; dashed line) under the hypothetical homogeneous material assumption.

enamel than in the dentin (Fig. 6). This occurs because enamel is more rigid than dentin (Young's modulus is about three times higher) and is subject to more bending stress because it forms the exterior surface of the tooth. Spears *et al*. (1993) point out the importance of anisotropy in enamel in reducing stress in teeth in their FEA, and propose that enamel perpendicular to its prism direction has a Young's modulus similar to dentin. Enamel would be more elastic parallel to the long axis of the tooth. This would reduce the bending stress in the enamel to the predictions of the HHM model (Fig. 6) and is further justification for using the HHM model. However, the ultimate tensile stress of enamel is much lower than that of dentin, and we expected cracks to form in the enamel first regardless of either the isotropy or anisotropy assumption. We observed that as the load increases, hairline cracks do appear as a series of fractures along the posterior edge of the tooth regularly spaced at about 0.5 mm apart.

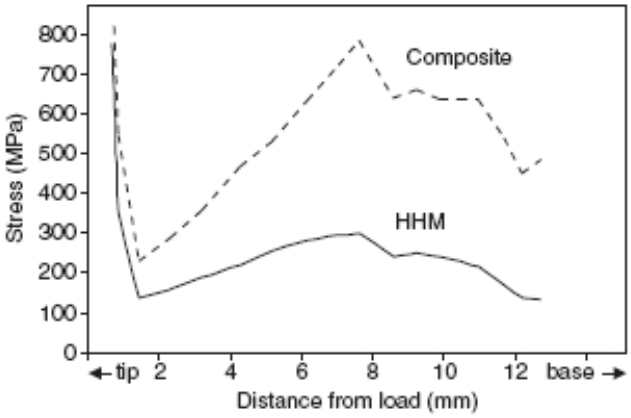

Figure 6 Comparison of predicted stresses along the shank of different models of teeth using finite-element analysis with a load of 1000N applied at the 70% point. The dashed line represents the tooth as a composite of enamel and dentin. The solid line represents the tooth as a hypothetical homogeneous material (HHM) where the stresses are greatly reduced.

Cracks do a remarkable job of concentrating stresses (Gordon, 1984), and once one is started in the enamel the whole tooth might be expected to break as the crack jumps to and continues into the dentin. If true, the whole tooth would fail when the weaker enamel fails. This does not occur. Considerably more force is needed before the whole tooth fails. Evidently, there is a crack-stopping mechanism that halts cracks at the dentin–enamel boundary (Imbeni *et al*., 2005). The interaction of enamel and dentin and crack propagation along the dentin–enamel boundary is an active area of research (Staninec *et al*., 2002; Imbeni *et al*., 2005 and references therein). Once the hairline cracks appear, our composite model of the tooth is no longer correct. This makes FEA and BTA of the composite structure problematic.

Calculation of $\sigma_{t,hu}$

The failure of the composite model meant that a descriptive model of tooth behavior under load was no longer possible; our goal became the development of the best possible predictive model of tooth strength. At this point we hit upon the idea of the homogeneous model (HHM). This model preserves information about the size and shape of the tooth (including the pulp cavity), but not the distribution of the enamel and dentin or the appearance of cracks in the enamel. Our calculated value of σt,hu is not the actual value experienced by the real tooth, but rather a hypothetical value based on our simplifying assumptions. We believe this hypothetical value can help us predict the real strength of teeth. For this approach to work, the basic shape and enamel/dentin composition of the teeth must be similar. This is clearly true within species; however, these similarities appear to hold true among the four species we experimentally tested (Fig. 1b). We would also expect similar values of $\sigma_{t,hu}$ across species if the HHM approach is valid. For the species we studied this appears to be correct (Fig. 2), although there is considerable variation in σt,hu. Ultimately the validity of the predictions based on the HHM model beyond

these four species will have to wait for future breaking tests on more species, particularly larger carnivores.

Under the HHM model, the teeth of adult animals fracture when maximal stress reaches about 338 MPa. To our surprise this value is strikingly greater than published $\sigma_{t,u}$ values for human and bovine dentin (~100 MPa) and enamel (~30 MPa; Staninec et al., 2002). This difference is surprising, given our method of treating the tooth as a single homogeneous material and the failure of the enamel under loading. Under such conditions we did not expect a value of σt,hu higher than dentin. There is often a fairly high range of values found for the $\sigma_{t,u}$ of dentin and enamel reported by researchers. Staninec et al. (2002) hypothesized that this high variance might be attributable to the variability of microfractures within the teeth. It should also be noted that Staninec *et al*. (2002) used a microfracture test where a sample of dentin was cut out of the tooth to be tested. Other studies have used the traditional hourglass approach, where again the sample specimen is cut out of the tooth (Sano *et al*., 1994). Classic experiments by Griffin (Gordon, 1984) indicated that typical glassware in the laboratory is 200 times weaker than theoretical expectations. Griffin's explanation, which was the foundation for modern fracture mechanics, was that small flaws in the glass greatly reduced its strength. Perhaps sample preparation introduces microfractures that contribute to the differences in our results with intact teeth. It is also possible that human and carnivore tooth material have significantly different strengths. Tests have shown that dentin strength within human teeth varies, depending on position and orientation. Human dentin near the pulp cavity has about half the tensile strength as dentin near the dentin–enamel junction (Staninec et al., 2002). Further tests are needed to address the differences of our ultimate stress values in carnivores and those found in human teeth. For our purpose of understanding tooth strength in carnivores, the breaking of whole teeth is more biologically relevant to actual breakage of teeth in the wild.

Comparing BTA and FEA

One of our goals was to test whether BTA was adequate for the analysis of canine teeth or is FEA needed. BTA and FEA give broadly similar results, but with differences we address here. The results from both analyses of a coyote tooth appear in Fig. 5, and it is representative of what we found across species. The large difference in predicted stresses near the point where force is applied is caused by the point load used in the FEA (although other methods of loading are possible). BTA assumes that point loads are distributed evenly across the beam's cross section at the point of load. As a result, BTA will not correctly model loads applied by a sharp point. FEA is much better at predicting such a spike of stress at the loading point. In our experiments we tried to reduce the problem of a local spike in stress at the load point by distributing the force applied to the tooth with a piece of leather inserted between indenter and tooth. If the load is spread over several adjacent nodes to emulate the action of the leather pad, the extreme spike in stress vanishes from the FEA and stresses near the load point converge with those from BTA. The load applied by the leather pad is neither the single point load we used in the FEA nor the diffuse load assumed by BTA; rather the load is spread over a small area by the leather's interaction with the surface of the tooth. Because we do not know what this actual distribution is, it cannot be specified and we cannot use the sophisticated power of FEA to model these near-load stresses accurately. As one might guess from looking at Fig. 5, there is a tendency for teeth to be crushed and to break at the point where load is applied, hence our use of the leather pad. In general few teeth broke at the indenter, attesting to the success of the leather pad. On occasion, because of the large forces involved, the leather pad failed to stop the indenter from crushing the tooth and breaking at the indenter. We were forced to disregard data where the teeth broke at the indenter because of problems in analyzing such breaks.

The second difference in BTA and FEA is potentially biologically important, although it had little impact on our analysis. Both BTA and FEA indicate that applying a load at the 70% position on a tooth never produces a maximal tensile stress at the base of the tooth. Rather it was always along the shank of the tooth (Fig. 1b). However, because of the shape of canines, errors in the predictions of BTA tend to increase towards the base of the tooth (Fig. 5). This error occurs because teeth are neither straight nor of uniform cross section, and this problem is largest at the base of the tooth. As an example, BTA overestimates tensile stress in the adult coyote model by about 40% near the tooth's base. Such a discrepancy will not impact our study because maximal stress is not found in this region of the tooth.

Otherwise, the results of FEA and BTA are similar. For the teeth we studied, the changes in cross-section size and shape were not large enough to invalidate the use of BTA in the shank of the tooth. These methods of analysis can be used interchangeably on simple teeth such as canines as long as stresses near the base do not need to be calculated. Our confidence in BTA here is reinforced by the results from FEA. We conclude that if BTA is to be used, the results must be verified using FEA. Given the greater power and the growing availability of FEA software, this method is preferable over BTA.

Modeling the strength of teeth

Results from regression analysis indicate that the relationship between body weight and tooth strength is allometric. Larger species have relatively weaker teeth. The tooth strength ($S_{A,0.7}$) of a fox-sized predator could support about 7.3 times its body weight, but for a lion-sized predator this value is about 4.4 times its body weight. Not surprisingly, the saber-toothed Smilodon is the most different species for tooth strength. The long tooth results in a much higher input arm that is not fully compensated for by the large cross-sectional area of the tooth. Our regression analysis predicts that a typical predator

of 320 kg has $S_{A,0.7}$ that could support about four times its body weight. Predictions from FEA for Smilodon indicate its $S_{A,0.7}$ could only support about 2.2 times its body weight (Fig. 4).

Acknowledgements

We thank the School of Natural Resources and the University of Nebraska State Museum, University of Nebraska-Lincoln for support, including specimens, and Angie Fox, Museum Technical Artist, for aid with the figures. Further we are especially grateful to Mark W. Beatty, Professor, and Bobby Simetich, Research Technologist, Biomaterials Section, College of Dentistry, University of Nebraska Medical Center, for the gracious use of their equipment and time. John Harris, Chief Curator, and Chris Shaw, Collection Manager, of the George C. Page Museum, a branch of the Los Angeles County Museum, kindly loaned us the Smilodon material. This is ARD research project # 15090.

References

Bowen, R.L. & Rodriquez, M.S. (1962). Tensile strength and modulus of elasticity of tooth structure and several restorative materials. *J. Am. Dent. Assoc.* 64, 378–387.

Craig, R.G. & Peyton, F.A. (1958). Elastic and mechanical properties of human dentin. *J. Dent. Res.* 37, 710–718.

Craig, R.G., Peyton, F.A. & Johnson, D.W. (1961). Compressive properties of enamel, dental cements, and gold. *J. Dent. Res.* 40, 936–945.

Gordon, J.E. (1984). *The new science of strong materials.* Princeton, NJ: Princeton.

Imbeni, V., Kruzic, J.J., Marshall, G.W., Marshall, S.J. & Ritchie, R.O. (2005). The dentin–enamel junction and the fracture of human teeth. *Nat. Mater.* 4, 229–232.

Knowlton, F.F. & Whittemore, S.L. (2001). Pulp cavity–tooth width ratios from known-age and wild-caught coyotes determined by radiography. *Wildl. Soc. Bull.* 29, 239–244.

Marshall, G.W. Jr., Balooch, M., Gallagher, R.R., Gansky, S.A. & Marshall, S.J. (2001). Mechanical properties of the dentinoenamel junction: AFM studies of nanohardness, elastic modulus, and fracture. J. Biomed. *Mater. Res*. 54, 87–95.

Mattheck, C. & Burkhardt, S. (1990). A new method of structural shape optimization based on biological growth. *Int. J. Fatigue* 12, 185–190.

Popov, E.P. (1999). *Engineering mechanic of solids.* New Jersey: Prentice-Hall.

Sano, H., Ciucchi, B., Matthews, W.G. & Pashley, D.H. (1994). Tensile properties of mineralized and demineralized human and bovine dentin. *J. Dent. Res.* 73, 1205–1211.

Spears, I.R, van Noort, R., Crompton, R.H., Cardew, G.E. & Howard, I.C. (1993). The effects of enamel anisotropy on the distribution of stress in a tooth. *J. Dent. Res.* 72, 1526–1531.

Staninec, M., Marshall, G.W., Hilton, J.F., Pashley, D.H., Gansky, S.A., Marshall, S.J. & Kinney, J.H. (2002). Ultimate tensile strength of dentin: evidence for a damage mechanics approach to dentin failure. *J. Biomed. Mater. Res.* 63, 342–345.

Van Valkenburgh, B. & Ruff, C.B. (1987). Canine tooth strength and killing behaviour in large carnivores. *J. Zool.* (Lond.) 212, 1–19.

Yettram, A.L., Wright, K.W.J. & Pickard, H.M. (1976). Finite element stress analysis of the crowns of normal and restored teeth. *J. Dent. Res.* 55, 1004–1011.